

Uncovering carbon burning in stars

A. TUMINO^{(1)(2)(*)}, C. SPITALERI⁽²⁾, M. LA COGNATA⁽²⁾, S. CHERUBINI⁽²⁾⁽³⁾,
G. L. GUARDO⁽⁴⁾, M. GULINO⁽¹⁾⁽²⁾, S. HAYAKAWA⁽⁵⁾, I. INDELICATO⁽²⁾,
L. LAMIA⁽²⁾⁽³⁾, H. PETRASCU⁽⁴⁾, R. G. PIZZONE⁽²⁾, S. M. R. PUGLIA⁽²⁾,
G. G. RAPISARDA⁽²⁾, S. ROMANO⁽²⁾⁽³⁾, M. L. SERGI⁽²⁾, R. SPARTÀ⁽²⁾⁽³⁾
and L. TRACHE⁽⁴⁾

⁽¹⁾ *Facoltà di Ingegneria e Architettura, Università “Kore” - Enna, Italy*

⁽²⁾ *INFN, Laboratori Nazionali del Sud - Catania, Italy*

⁽³⁾ *Dipartimento di Fisica e Astronomia, Università degli Studi di Catania - Catania, Italy*

⁽⁴⁾ *Horia Hulubei National Institute for R&D in Physics and Nuclear Engineering - Bucharest-Magurele, Romania*

⁽⁵⁾ *Center for Nuclear Studies, The University of Tokyo - Tokyo, Japan*

received 5 February 2019

Summary. — Carbon burning takes place in stars at deep sub-Coulomb energies through the $^{12}\text{C}(^{12}\text{C},\alpha)^{20}\text{Ne}$ and $^{12}\text{C}(^{12}\text{C},p)^{23}\text{Na}$ reactions. Here we report the first measurement of these reactions at the relevant energies via the Trojan Horse Method off the deuteron in ^{14}N . In particular, the $^{12}\text{C} + ^{12}\text{C}$ fusion has been measured from $E_{c.m.}=2.7$ MeV down to 0.8 MeV. This range of energies is relevant for several astrophysical scenarios, from superburst ignition to quiescent burning. The astrophysical $S(E)$ factors reveal several resonances, which are responsible for a very large increase of the reaction rate at the relevant temperatures.

1. – Introduction

The $^{12}\text{C}+^{12}\text{C}$ fusion is one of the most important reactions in Nuclear Astrophysics and has a key role in a broad range of scenarios in carbon rich environments. In particular, it strongly influences star evolution and nucleosynthesis of intermediate mass stars (8-10 M_{\odot}) and up with more than 10 M_{\odot} [1]. It determines also the lower stellar mass limit for carbon ignition. This limit separates the progenitors of white dwarfs, novae and type Ia supernovae, from those of core-collapse supernovae, neutron stars, and stellar mass black holes; it constrains superbursts model with neutron and strange stars, in particular if resonances are found to contribute in the Gamow peak [2]; it influences the weak component of the s process which produce the elements between Fe and Sr. The

(*) E-mail: tumino@lns.infn.it

temperatures for carbon burning range from 0.8 to 1.2 GK, corresponding to center-of-mass energies from 1 to 3 MeV. The Coulomb barrier height for the $^{12}\text{C}+^{12}\text{C}$ system is around 6 MeV, much higher than the energies of interest. In that region, the cross section falls rapidly below the nanobarns. That is why the measurement of the cross section at astrophysical energies remains a difficult task. The excitation energy of the compound nucleus ^{24}Mg is high enough to decay by particle emission. Alpha, proton and neutron are the dominant evaporation channels, leading respectively to ^{20}Ne , ^{23}Na and ^{23}Mg , which can also be produced in excited bound states. Below a center of mass energy E_{cm} of 2.5 MeV there is not enough energy to feed ^{23}Mg even in its ground state and α and p channel are the only relevant ones at low energies. Considerable efforts have been devoted to measure the $^{12}\text{C}+^{12}\text{C}$ cross section at astrophysical energies, involving both, charged particle [3-5] and gamma ray spectroscopy [6-11]. Nevertheless, it has only been previously measured down to $E_{cm} = 2.5$ MeV, still at the beginning of the region of astrophysical interest. However, below $E_{cm} = 3.0$ MeV the reported cross sections disagree and are rather uncertain, because at these energies the presence of ^1H and ^2H contamination in the C targets hampered the measurement of the $^{12}\text{C}+^{12}\text{C}$ process both in particle and gamma ray studies. In a more recent study [12], the astrophysical $S(E)$ factor exhibits new resonances at $E_{cm} \leq 3.0$ MeV, in particular, a strong resonance at $E_{cm} = 2.14$ MeV, which lies at the high-energy tail of the Gamow peak. This resonance, if confirmed, would increase the present nonresonant reaction rate of the alpha channel by a factor of 5 near $T = 0.8$ GK. On the other hand, it has been proposed that a sub-barrier fusion hindrance effect might drastically reduce the reaction rate at astrophysical energies. As known, measurements at lower energies are extremely difficult. Moreover, in the present case the extrapolation procedure from current data to the ultra-low energies is complicated by the presence of possible resonant structures even in the low-energy part of the excitation function. Thus, further measurements extending down to at least 1 MeV would be extremely important. In this paper, we are going to discuss the indirect study of the $^{12}\text{C}(^{12}\text{C},\alpha)^{20}\text{Ne}$ and $^{12}\text{C}(^{12}\text{C},p)^{23}\text{Na}$ reactions via the Trojan Horse Method (THM) applied to the $^{12}\text{C}(^{14}\text{N},\alpha)^{20}\text{Ne}^2\text{H}$ and $^{12}\text{C}(^{14}\text{N},p)^{23}\text{Na}^2\text{H}$ three-body processes in the quasi-free (QF) kinematics regime, where ^2H from the ^{14}N nucleus is spectator to the $^{12}\text{C}+^{12}\text{C}$ two-body processes [13]. There is a number of works providing evidence of direct ^{12}C transfer in the $^{12}\text{C}(^{14}\text{N},d)^{24}\text{Mg}^*$ reaction at 30 MeV of beam energy and up [14, 15].

2. – Short description of the Trojan Horse Method

The Trojan Horse Method (THM) [16-18] is a valid alternative approach to determine the bare nucleus $S(E)$ factor for rearrangement reactions. The THM considers the QF contribution of an appropriate three-body reaction $A + a \rightarrow c + C + s$ performed at energies well above the Coulomb barrier to obtain the cross section of a charged particle two-body process $A + x \rightarrow c + C$ at low energies, relevant for astrophysics. To this aim, the nuclear reaction theory is applied assuming that the nucleus a can be described in terms of the $x \oplus s$ cluster structure. Thanks to the high energy in the $A + a$ entrance channel, the two body interaction can be considered as taking place inside the nuclear field, without experiencing either Coulomb suppression or electron screening effects. The $A + a$ relative motion is compensated for by the $x - s$ binding energy, determining the so called "quasi-free two-body energy" given by

$$(1) \quad E_{q.f.} = E_{Aa} - B_{x-s}$$

where E_{Aa} represents the beam energy in the center-of-mass system and B_{x-s} is the binding energy for the $x-s$ system. Then, a cutoff in the momentum distribution, which is related to the Fermi motion of s inside the Trojan-horse a , fixes the range of energies around the "quasi-free two-body energy" accessible in the astrophysical relevant reaction. In the Impulse Approximation either in Plane Wave or in Distorted Wave (this does not change the energy dependence of the two-body cross section but only its absolute magnitude), the three body-cross cross section can be factorized as:

$$(2) \quad \frac{d^3\sigma}{dE_c d\Omega_c d\Omega_C} \propto [KF |\varphi_a(\mathbf{p}_{sx})|^2] \left(\frac{d\sigma}{d\Omega_{c.m.}} \right)^{\text{HOES}}$$

where KF is a kinematical factor containing the final state phase-space factor. It is a function of the masses, momenta and angles of the outgoing particles; $\varphi_a(\mathbf{p}_{sx})$ is proportional to the Fourier transform of the radial wave function $\chi(\mathbf{r})$ for the $x-s$ inter-cluster relative motion; $(d\sigma/d\Omega_{c.m.})^{\text{HOES}}$ is the half-off-energy-shell (HOES) differential cross section for the binary reaction at the center of mass energy $E_{c.m.}$ given in post-collision prescription by

$$(3) \quad E_{c.m.} = E_{cC} - Q_{2b} .$$

Here, Q_{2b} is the Q -value of the binary reaction and E_{cC} is the relative energy of the outgoing particles c and C .

The THM has been applied to many direct and resonant processes relevant for nuclear astrophysics, usually involving light particles as spectators, such as d , ${}^3\text{He}$, ${}^6\text{Li}$ ([19-29] and references therein). This is the first application of the THM to heavy ion reactions.

3. – The Experiment

The experiment was performed at the INFN - Laboratori Nazionali del Sud. A ${}^{14}\text{N}$ beam accelerated at 30 MeV by the SMP TANDEM was delivered onto a $100 \mu\text{g}/\text{cm}^2$ C target with a beam spot on target smaller than 1.5 mm. The experimental setup consisted of two telescopes (38 μm silicon detector as ΔE - and 1000 μm position sensitive detector (PSD) as E-detector) placed on both sides with respect to the beam direction in symmetric configuration (two on each side), covering angles from 7° to 30° . The ejectile of the two-body reactions (either α or p) was detected in coincidence with the spectator d particle. The heavy counterparts in the two-body reactions have quite low energy and, if detected, this would imply a high detection threshold. In order to fulfil the QF requirement for the spectator d particle to be essentially part of the beam, this particle was detected at forward angles. The angular regions covered by the detectors were optimized for the QF kinematics of the break-up process of interest, and the investigated range of deuteron momentum values was feasible to check the existence of the QF mechanism.

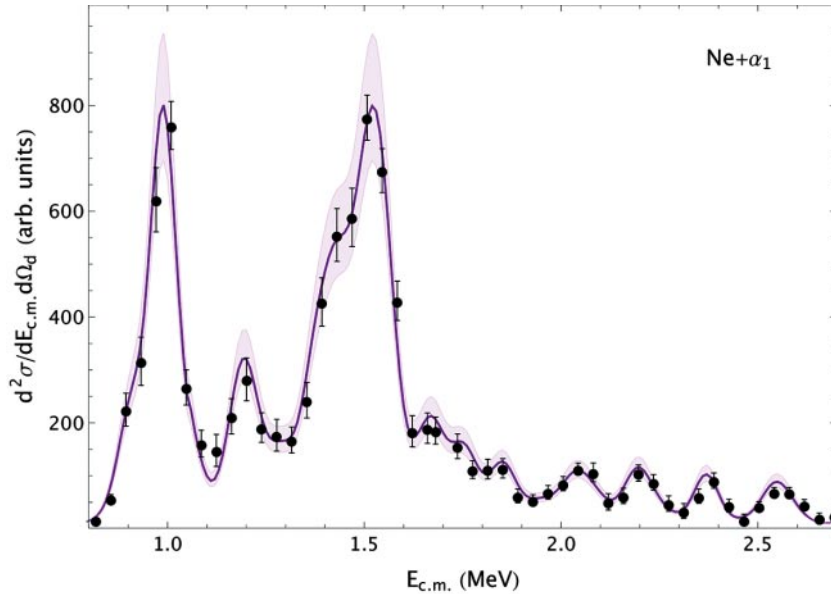


Fig. 1. – Quasi-free two-body cross section for the $^{20}\text{Ne}+\alpha_1$ channel (black filled dots). The solid purple line is the result of R-matrix calculations. The light purple band takes into account the uncertainties of the resonance parameters, including correlations.

4. – Results and discussion

Several steps are involved in the data analysis (see [13]) and after their completion the two-body cross section of astrophysical relevance was extracted for four channels: $^{20}\text{Ne}+\alpha_0$, $^{20}\text{Ne}+\alpha_1$, $^{23}\text{Na}+p_0$ and $^{23}\text{Na}+p_1$. The yield for the $^{20}\text{Ne}+\alpha_1$ channel is shown in Fig. 1 (black solid dots) projected onto the $^{12}\text{C}+^{12}\text{C}$ relative energy variable, $E_{c.m.}$.

A modified one-level many-channel R-matrix analysis was carried out including the ^{24}Mg states reported in [13]. Taking advantage of the α_1 and p_1 fractions of the total fusion yield observed at $E_{c.m.}$ below 2.8 MeV [5,12] and reported in [12], one can estimate the lower limits of the $\alpha_0+\alpha_1$ and p_0+p_1 contributions to the total cross sections from the present experiment at the highest energies as 0.85 ± 0.07 and 0.68 ± 0.06 , respectively. However, moving from $E_{c.m.}=2.8$ to 1.5 MeV, the number of accessible excited states for both ^{20}Ne and ^{23}Na already reduces to half and the cross sections for ^{20}Ne and ^{23}Na excited states drop steeper than those for ground states, due to the sharper decrease by orders of magnitude of the corresponding penetration factors. According to the results of [5] at $E_{c.m.}\leq 3$ MeV, and monitoring the decrease of the penetration factors for the relevant states, the fraction of the total fusion yield from α and p channels other than $\alpha_{0,1}$ and $p_{0,1}$ was neglected in the modified R-matrix analysis with estimated errors at $E_{c.m.}$ below 2 MeV lower than 1% and 2% for the α and p channels, respectively. The result for the $^{20}\text{Ne}+\alpha_1$ channel is shown in Fig. 1 as middle solid purple line with light purple band arising from the uncertainties on the resonance parameters, including correlations. The resonance structure observed in the excitation functions is consistent with ^{24}Mg resonance energies reported in the literature with some tendency for the even J states to be clustered at about 1.5 MeV and this might be a sign of intermediate structure

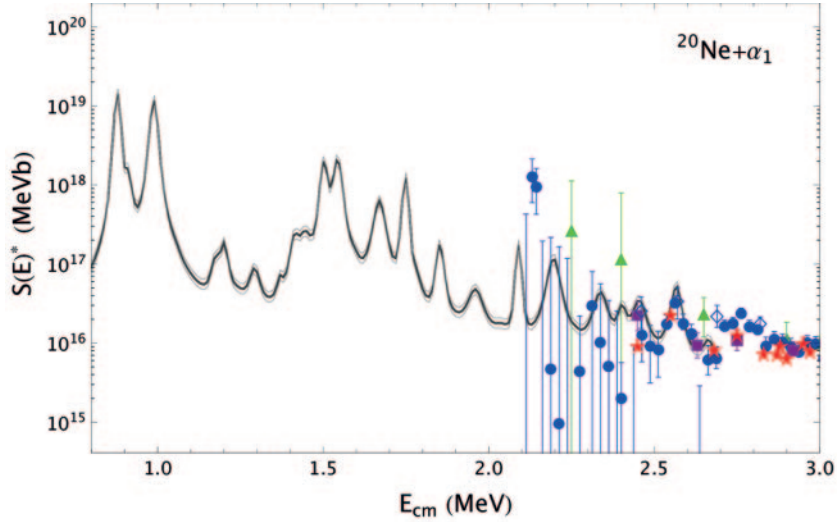


Fig. 2. – THM astrophysical $S(E)^*$ factor for the $^{20}\text{Ne}+\alpha_1$ channel (black solid line). The grey band represents the region spanned by R-matrix calculations with lower and upper values of the resonance parameters. Available direct data in the investigated $E_{c.m.}$ range are reported as purple filled squares [3], blue empty diamonds [6], red filled stars [7], blue filled circles [12] and green filled triangles [30].

of ^{24}Mg associated with a $^{12}\text{C}+^{12}\text{C}$ molecular configuration. The THM reduced widths thus entered a standard R-matrix code and the $S(E)$ factors for the four reaction channels were determined.

The results are shown in Fig. 2 for the $^{20}\text{Ne}+\alpha_1$ in terms of modified $S(E)$ factor, $S(E)^*$, as it is customary for most of the previous investigations [11,12]. The black middle line and the grey band represent the best fit curve and the range defined by the total uncertainties, respectively. The grey band is the result of R-matrix calculations with lower and upper values of the resonance parameters provided by their errors.

The resonant structures are superimposed onto a flat nonresonant background taken from [12] for all channels and quoted as 0.4×10^{16} MeVb. Unitarity of the S-matrix is guaranteed within the experimental uncertainties. Normalization to direct data was done in the $E_{c.m.}$ window 2.5-2.63 MeV of the $^{20}\text{Ne}+\alpha_1$ channel where a sharp resonance corresponding to the level of ^{24}Mg at 16.5 MeV shows up and available data [12,3,6,7] in this region are the most accurate among those available in the full overlapping region with THM data. Scaling to the resonance by means of a weighted normalization, the resulting normalization error is 5% that enters the definition of the grey band of Fig. 2, combined in quadrature with errors on the resonance parameters.

All the existing direct data below $E_{c.m.} = 3$ MeV are shown as blue filled circles [12], purple filled squares [3], blue empty diamonds [6], red filled stars [7] and green filled triangles [30]. Except for the data from [12], their low energy limit is fixed by background due to hydrogen contamination in the targets. Disregarding these cases, agreement between THM and direct data is apparent within the experimental errors except for the direct low-energy limit around 2.14 MeV, where THM data do not confirm the claim of a strong resonance, rather a nearby one at 2.095 MeV about one order of magnitude less

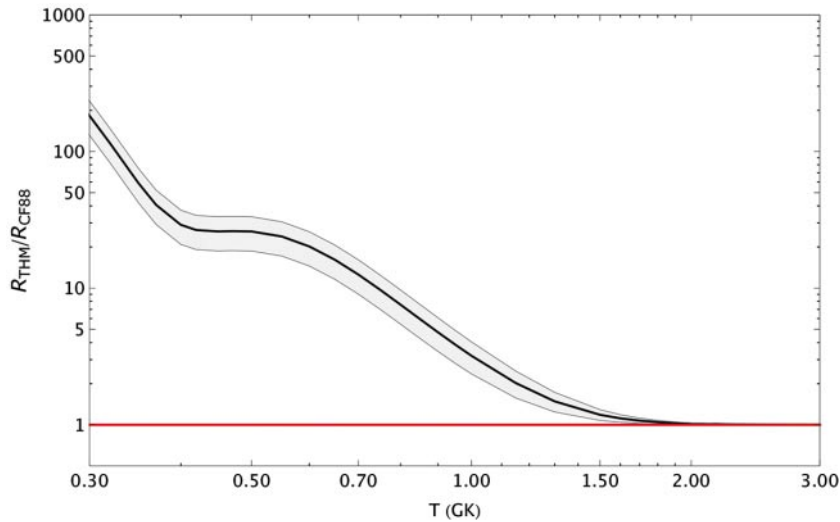


Fig. 3. – Ratio between the total THM $^{12}\text{C}+^{12}\text{C}$ reaction rate (black line) and the reference one (red line) from [36]. The grey shading defines the region spanned owing to the $\pm 1\sigma$ uncertainties.

intense in the $^{20}\text{Ne}+\alpha_1$ channel (see Fig. 2) and with similar intensity in the $^{23}\text{Na}+p_1$ one. The present result is in agreement with spectroscopy studies of [31, 32] with a deep at 2.14 MeV and no particularly strong α state around 2.1 MeV. Further agreement is found with the unpublished experimental data down to $E_{c.m.}=2.15$ MeV from [33] for the $^{12}\text{C}(^{12}\text{C}, p_{0,1})^{23}\text{N}$ reactions. Our result is also consistent within experimental errors with the total $S(E)^*$ from a recent experiment at higher energies [34] calculated at the overlapping $E_{c.m.}$ value of 2.68 ± 0.08 MeV.

The reaction rates for the four processes were calculated from the THM $S(E)^*$ factors using the standard formula reported in [35]. Since the total $^{12}\text{C}+^{12}\text{C}$ fusion yield at $E_{c.m.}$ below 2.8 MeV is likely to be exhausted by the $\alpha_{0,1}$ and $p_{0,1}$ channels (see Methods), we assume that the sum of their reaction rates in the $E_{c.m.}$ range here investigated is representative of the total one.

The reaction rate is shown in Fig. 3 divided by the reference rate from [36]. It experiences a variation below 2 GK with an increase from a factor of 1.18 at 1.2 GK to a factor of more than 25 at 0.5 GK.

The latter increase, due mainly to the resonant structure around $E_{c.m.}=1.5$ MeV, endorses the fiducial value conjectured in [37] to reduce down to a factor of 2 the theoretical superburst ignition depths in accreting neutron stars for a realistic range of crust thermal conductivities and core Urca neutrino emissivities. This change is compatible with the observationally inferred superburst ignition depths. In other words, carbon burning can trigger superbursts. As for the hydrostatic carbon burning regime (0.6 to 1.2 GK), the present rate change will lower temperatures and densities at which ^{12}C ignites in massive post-main-sequence stars. Profiting of the stellar modeling reported in [38], for core C-burning of a star of $25M_{\odot}$, the ignition temperature and density would undergo a decrease of down to 10% and 30% respectively. This is just a taste of the impact that the new $^{12}\text{C}+^{12}\text{C}$ reaction rate has in the various astrophysical contexts and further discussion needs much work.

REFERENCES

- [1] GARCIA-BERRO E., et al., *Astrophys. J.*, **485**, (1997) 765.
- [2] COOPER R.L., et al., *Astrophys. J.*, **702**, (2009) 660.
- [3] MAZARAKIS M.G. & STEPHENS W.E., *Phys. Rev. C*, **7** (1973) 1280.
- [4] PATTERSON J.R., WINKLER H. and ZAIDINS C.S., *Astrophys. J.* **157** (1969) 367.
- [5] BECKER H.W., KETTNER K.U., ROLFS C. and TRAUTVETTER H.P., *Z. Phys. A*, **303** (1981) 305.
- [6] HIGH M.D., CUJEC B., *Nucl. Phys. A*, **282** (1977) 181.
- [7] KETTNER K.U., LORENZ-WIRZBA H. and ROLFS C., *Z. Phys. A* **298** (1980) 65.
- [8] ROSALES P., et al., *Rev. Mex. Phys.* **49** S4 (2003) 88.
- [9] BARRÓN-PALOS L., et al., *Nucl. Phys. A* **779** (2006) 318.
- [10] BARRÓN-PALOS L., et al. *Eur. Phys. J. A* Direct (2005), doi:10.1140/epjad/i2005-06-008-2.
- [11] AGUILERA E.F., et al., *Phys. Rev. C* **73** (2006) 064501.
- [12] SPILLANE T., et al., *Phys. Rev. Lett.* **98**, (2007) 122501.
- [13] TUMINO A., et al., *Nature* **557**, (2018) 687.
- [14] ARTEMOV K.P., et al., *Phys. Lett. B*, **149** (1984) 325.
- [15] ZURMUEHLE R.W., et al., *Phys. Rev. C* **49** (1994) 2549.
- [16] SPITALERI C., et al., *Phys. At. Nucl.*, **74**, (2011) 1763.
- [17] TUMINO A., et al., *Few Body Syst.*, **54**, Issue 5-6 (2013) 745.
- [18] TRIBBLE R., et al., *Rep. Prog. Phys.*, **77**, Issue: 10 (2014) 106901.
- [19] RINOLLO A., et al., *Nucl. Phys. A*, **758** (2005) 146.
- [20] PIZZONE R.G., et al., *A&A* **438** (2005) 779.
- [21] ROMANO S., et al., *Eur. Phys. J. A* **27** (2006) 221.
- [22] LA COGNATA M., et al., *Phys. Rev. Lett.* **101** (2008) 152501.
- [23] TUMINO A., et al., *Phys. Rev. Lett.* **98** (2007) 252502.
- [24] TUMINO A., et al., *Phys. Rev. C* **78** (2008) 064001.
- [25] TUMINO A., et al., *Phys. Lett. B* **700** (2011) 111.
- [26] TUMINO A., et al. *Phys. Lett. B* **705** (2011) 546.
- [27] LAMIA L., et al., *Astrophysical J.* **768**, (2013) 65.
- [28] TUMINO A., et al. *Astrophysical J.* **785** (2014) 96.
- [29] CHENGBO LI, et al. *Phys. Rev. C* **92** (2015) 025805.
- [30] BARRÓN-PALOS L., et al., *Nucl. Phys. A* **779** (2006) 318.
- [31] ABEGG R. and DAVIS C.A., *Phys. Rev. C* **43** (1991) 6.
- [32] CACIOLLI A., et al., *NIM B* **266** (2008) 1932.
- [33] ZICKEFOOSE J., *Phys. Rev. C* **97** (2018) 065806.
- [34] JIANG C.L., et al., *Phys. Rev. C* **97** (2018) 012801(R).
- [35] ILIADIS C., *Nuclear Physics of Stars.* (2007), WILEY- VCH Verlag GmbH & Co. KGaA, Weinheim).
- [36] CAUGHLAN G.R. and FOWLER W.A., *At. Data Nucl. Data Tables* **40**, (1988) 283.
- [37] COOPER R.L., et al., *Astrophysical J.* **702** (2009) 660.
- [38] PIGNATARI M., et al., *Astrophys. J.* **762** (2013) 31.